Hindawi
Discrete Dynamics in Nature and Society
Volume 2018, Article ID 2950357, 8 pages
https://doi.org/10.1155/2018/2950357

Research Article

On the Q–S Chaos Synchronization of Fractional-Order Discrete-Time Systems: General Method and Examples

Adel Ouannas,[1] Amina-Aicha Khennaoui,[2] Giuseppe Grassi,[3] and Samir Bendoukha[4]

[1] *Mathematics and Computer Science Department, Tebessa University, 12062, Algeria*
[2] *Department of Mathematics and Computer Sciences, University of Larbi Ben M'hidi, Oum El Bouaghi, Algeria*
[3] *Universita del Salento, Dipartimento Ingegneria Innovazione, 73100 Lecce, Italy*
[4] *Department of Electrical Engineering, College of Engineering, Yanbu, Taibah University, Saudi Arabia*

Correspondence should be addressed to Samir Bendoukha; sbendoukha@taibahu.edu.sa

Received 19 May 2018; Accepted 6 August 2018; Published 10 September 2018

Academic Editor: Allan C. Peterson

In this paper, we propose two control strategies for the Q–S synchronization of fractional-order discrete-time chaotic systems. Assuming that the dimension of the response system m is higher than that of the drive system n, the first control scheme achieves n-dimensional synchronization whereas the second deals with the m-dimensional case. The stability of the proposed schemes is established by means of the linearization method. Numerical results are presented to confirm the findings of the study.

1. Introduction

Since the concept of chaos synchronization was first proposed nearly three decades ago, dynamical systems exhibiting chaotic behavior have attracted considerable attention in a number of fields. In addition to the original continuous-time chaotic systems such as Lorenz and Chen systems, discrete-time chaotic systems or maps have been proposed and studied. Among the most widely used 2-component discrete systems of these are the Hénon map [1], the Lozi map [2], and the flow model [3]. Higher-dimensional systems have also been studied such as the generalized Hénon map [4] and the Stefanski map [5]. All of these maps are classified as integer–order signifying that the difference order is integer.

Although fractional calculus was studied by mathematicians as early as the nineteenth century, it wasn't until recently that it gained popularity in applied science and engineering. For the longest time, the study and application of fractional calculus was limited to continuous time. However, most recently, researchers have diverted their attention to the discrete-time case and attempted to put together a complete theoretical framework for the subject. Perhaps one of the earliest works is that of [6]. Among the most interesting and relevant works on fractional discrete calculus in the last decade is that of [7] where the authors introduce a backward fractional difference operator. In [8], the author discusses the discrete-time difference counterparts of conventional Riemann and Caputo derivatives. More on the general notation of fractional discrete-time calculus can be found in [9, 10]. Furthermore, the numerical formulas corresponding to a fractional difference systems can be found in [11]. Recent studies have examined the stability conditions for fractional discrete-time systems including [12]. Most recently, some advances have been made in relation to chaotic fractional discrete-time systems and their applications. A number of fractional difference maps including the fractional logistic map [13], the fractional sine map [14], fractional Hénon map [15], and fractional cubic logistic map [16].

Chaos synchronization in its simplest form refers to the control of a response chaotic system to force its trajectory towards that of a drive [17]. In this case, the error defined as the difference between the states of the drive and those of the response towards zero as $t \longrightarrow \infty$. Numerous other types of synchronization have been proposed in the literature, whereby a general function of the two state vectors is forced to zero instead. The synchronization of integer–order discrete-time systems subject to different definitions of the error has been studied in the literature such as hybrid synchronization

[18], generalized synchronization [19], and inverse full state hybrid projective synchronization [20]. As for fractional-order discrete systems, the literature related to their synchronization is still very limited including synchronization of the logistic map [21], synchronization based on the stability condition [22], synchronization of linearly coupled fractional Hénon maps [23], and impulsive synchronization of fractional-order discrete-time hyperchaotic systems [24].

In this paper, we are concerned with the Q–S synchronization of fractional-order discrete-time chaotic systems with different dimensions and non–identical orders. In this scheme, two functions Q and S are used to condition the response and drive states, respectively, such that different values for Q and S lead to different types of synchronization. Q–S synchronization was first proposed by Yan in 2005 [25] for continuous–time dynamical systems. The author developed a backstepping approach with a strict feedback form to synchronize two identical systems. The author, then, extended the Q–S scheme to discrete-time systems [26]. In the years that followed, several algorithms were proposed for the Q–S synchronization of integer-order continuous-time systems including [27–29]. Several studies also looked at the fractional continuous-time case such as [30]. Finally, in [31, 32], the authors investigated Q–S synchronization between integer-order and fractional-order continuous-time systems with different dimensions.

In the next section of this paper, we will present the notation adopted in our study and formulate the Q–S synchronization problem for a fractional-order discrete-time chaotic drive-response pair. We denote the number of states for the drive and response by n and m, respectively. Sections 3 and 4 present the control laws for the m–dimensional and n–dimensional cases, respectively. Section 5 presents some numerical results related to two particular examples. Finally, Section 6 provides a general summary of the main findings of this study.

2. Problem Formulation

Consider the following drive and response maps described as

$$\begin{aligned} {}^{C}\Delta_a^{\alpha} X(t) &= AX(t+\upsilon-1) + f(X(t+\upsilon-1)), \\ &\qquad \forall t \in \mathbb{N}_{a+1-\alpha}, \\ {}^{C}\Delta_a^{\beta} Y(t) &= BY(t+\upsilon-1) + g(Y(t+\upsilon-1)) + U, \\ &\qquad \forall t \in \mathbb{N}_{a+1-\beta} \end{aligned} \tag{1}$$

where $X(t) = (x_1(t), \ldots, x_n(t))^T$ and $Y(t) = (y_1(t), \ldots, y_m(t))^T$ denote the drive and response state vectors, respectively, $A \in \mathbb{R}^{n\times n}$, $B \in \mathbb{R}^{m\times m}$, $f : \mathbb{R}^n \longrightarrow \mathbb{R}^n$, $g : \mathbb{R}^m \longrightarrow \mathbb{R}^m$ are nonlinear functions and $U = (u_i)_{1\le i\le m}$ is a vector controller to be determined by the control laws of the synchronization scheme. Note that $\mathbb{N}_a$ denotes the set of natural numbers starting from a and $0 < \upsilon \le 1$.

The notation ${}^{C}\Delta_a^{\upsilon} X(t)$ denotes the Caputo type delta difference of $X(t)$ defined over $\mathbb{N}_a$ [8]. This operator can be defined as

$$\begin{aligned} {}^{C}\Delta_a^{\upsilon} X(t) &= \Delta_a^{-(n-\upsilon)} \Delta^n X(t) \\ &= \frac{1}{\Gamma(n-\upsilon)} \sum_{s=a}^{t-(n-\upsilon)} (t-s-1)^{(n-\upsilon-1)} \Delta_s^n X(s), \end{aligned} \tag{2}$$

for $\upsilon \notin \mathbb{N}$, $t \in \mathbb{N}_{a+n-\upsilon}$, and $n = [\upsilon] + 1$. The operator $\Delta_s^n X(t)$ denotes the υ–th fractional sum of $x_i : \mathbb{N}_a \longrightarrow \mathbb{R}$ defined in [7] as

$$\Delta_a^{-\upsilon} X(t) = \frac{1}{\Gamma(\upsilon)} \sum_{s=a}^{t-\upsilon} (t-s-1)^{(\upsilon-1)} X(s), \tag{3}$$

with $\upsilon > 0$, $\mathbb{N}_a = \{a, a+1, a+2, \ldots\}$, and $t^{(\upsilon)}$ is given in terms of the Gamma function Γ as

$$t^{(\upsilon)} = \frac{\Gamma(t+1)}{\Gamma(t+1-\upsilon)}. \tag{4}$$

For the purpose of this study, we will assume $a = 0$ and thus the subscript may be ignored. With these notations in mind, we can go ahead and define the Q–S synchronization of our drive-response pair. The following definition is consistent with the literature reviewed earlier in this paper.

Definition 1. The drive-response pair (1) is Q–S synchronized in the dth dimension if there exist a controller $U = (u_i)_{1\le i\le m}$ and two functions $Q : \mathbb{R}^m \longrightarrow \mathbb{R}^d$ and $S : \mathbb{R}^n \longrightarrow \mathbb{R}^d$ such that

$$\lim_{t\longrightarrow+\infty} \|e(t) := Q(Y(t)) - S(X(t))\| = 0. \tag{5}$$

It is easy to observe from Definition 1 that, depending on our choice of the pair $(Q(Y(t)), S(X(t)))$, we may end up with one of many synchronization types, namely,

$$\begin{gathered} (Y(t), X(t)) \longrightarrow \text{Complete synchronization}, \\ (Y(t), -X(t)) \longrightarrow \text{Anti synchronization}, \\ (Y(t), \theta X(t)), \quad \theta \in \mathbb{R}^* \longrightarrow \\ \text{Projective synchronization}, \\ (Y(t), MX(t)), \quad M \in \mathbb{R}^{m\times n} \longrightarrow \\ \text{Matrix projective synchronization}, \\ (MY(t), X(t)), \quad M \in \mathbb{R}^{n\times m} \longrightarrow \\ \text{Inverse matrix projective synchronization}, \\ (Y(t), S(X(t))) \longrightarrow \\ \text{Generalized synchronization}, \\ (Q(Y(t)), X(t)) \longrightarrow \\ \text{Inverse generalized synchronization}. \end{gathered} \tag{6}$$

For reasons that will become clear later on, suppose that Q can be divided into two parts:

$$Q(Y(t)) = \mathbf{Q}Y(t) + \mathbf{q}(Y(t)), \tag{7}$$

where $\mathbf{Q}$ is an invertible $d \times d$ matrix and $\mathbf{q} : \mathbb{R}^d \longrightarrow \mathbb{R}^d$ is a nonlinear function. In the following two sections, we will present two distinct synchronization schemes of dimensions $d = m$ and $d = n$, respectively.

3. Q–S Synchronization in Dimension m

The Q–S synchronization error defined in (5) can be written in the following form:

$$e(t) = \mathbf{Q}Y(t) + \mathbf{q}(Y(t)) - S(X(t)), \tag{8}$$

where $\mathbf{Q}$ is an invertible $m \times m$ matrix, $\mathbf{q} : \mathbb{R}^m \longrightarrow \mathbb{R}^m$, and $S : \mathbb{R}^n \longrightarrow \mathbb{R}^m$. The β order Caputo fractional difference of (8) is of the following form:

$$\begin{aligned}
{}^C\Delta^\beta e(t) &= {}^C\Delta^\beta [\mathbf{Q}Y(t) + \mathbf{q}(Y(t)) - S(X(t))] \\
&= {}^C\Delta^\beta [\mathbf{Q}Y(t)] + {}^C\Delta^\beta \mathbf{q}(Y(t)) - {}^C\Delta^\beta S(X(t)) \\
&= \mathbf{Q}{}^C\Delta^\beta Y(t) + {}^C\Delta^\beta \mathbf{q}(Y(t)) - {}^C\Delta^\beta S(X(t)) \\
&= \mathbf{Q}[BY(t+\beta-1) + g(Y(t+\beta-1)) + U] \\
&\quad + {}^C\Delta^\beta \mathbf{q}(Y(t)) - {}^C\Delta^\beta S(X(t)) \\
&= \mathbf{Q}BY(t+\beta-1) + \mathbf{Q}g(Y(t+\beta-1)) + \mathbf{Q} \\
&\quad \times U + {}^C\Delta^\beta \mathbf{q}(Y(t)) - {}^C\Delta^\beta S(X(t)).
\end{aligned} \tag{9}$$

This can be further simplified to

$${}^C\Delta^\beta e(t) = (B - C)e(t+\beta-1) + \mathbf{R} + \mathbf{Q} \times U, \tag{10}$$

where $C \in \mathbb{R}^{m\times m}$ is an appropriately chosen control matrix and

$$\begin{aligned}
\mathbf{R} = (C - B)e(t) + \mathbf{Q}BY(t) + \mathbf{Q}g(Y(t)) \\
+ {}^C\Delta^\beta \mathbf{q}(Y(t)) - {}^C\Delta^\beta S(X(t)).
\end{aligned} \tag{11}$$

The following remark is important.

Remark 2. Note that our aim in synchronization is to find a suitable controller U that forces the synchronization error to zero asymptotically. Since U is part of the response system, the function $Q(Y(t))$ hinders our process. To overcome this problem, we assumed that $Q(Y(t))$ can be decomposed into a linear part (matrix $\mathbf{Q}$) and some other nonlinear function $\mathbf{q}(Y(t))$. The reasoning behind this is that matrix $\mathbf{Q}$ is constant and thus may be factored out of the fractional difference operator.

Before stating the proposed control law and establishing its stability, it is important to state the following theorem, which is essential for our proof. Interested readers are referred to [33] for the proof of this result.

Theorem 3. *The zero equilibrium of the linear fractional-order discrete-time system:*

$${}^C\Delta_a^\upsilon e(t) = \mathbf{M}e(t+\upsilon-1), \tag{12}$$

where $e(t) = (e_1(t), \ldots, e_n(t))^T$, $0 < \upsilon \le 1$, $\mathbf{M} \in R^{n\times n}$ and $\forall t \in \mathbb{N}_{a+1-\upsilon}$, is asymptotically stable, if

$$\begin{aligned}
\lambda \in \left\{ z \in \mathbb{C} : |z| < \left(2\cos\frac{|\arg z| - \pi}{2-\upsilon}\right)^\upsilon \text{ and } |\arg z| \right. \\
\left. > \frac{\upsilon\pi}{2} \right\},
\end{aligned} \tag{13}$$

for all the eigenvalues λ of $\mathbf{M}$.

With this stability result, we are now ready to present our synchronization scheme.

Theorem 4. *The drive-response pair (1) is globally Q–S synchronized in dimension m subject to*

$$U = -\mathbf{Q}^{-1} \times \mathbf{R}, \tag{14}$$

where $\mathbf{Q}^{-1}$ is the inverse of $\mathbf{Q}$ and the control matrix C is selected such that all the eigenvalues λ of $B - C$ satisfy

$$-2^\beta < \lambda < 0. \tag{15}$$

Proof. By substituting (14) into (10), we obtain a new formulation for the error system:

$${}^C\Delta^\beta e(t) = (B - C)e(t+\beta-1). \tag{16}$$

Now, it is easy to see that subject to (15), all eigenvalues λ of matrix $B - C$ satisfy

$$|\arg\lambda| = \pi > \frac{\beta\pi}{2}, \tag{17}$$

and

$$|\lambda| < \left(2\cos\frac{|\arg\lambda| - \pi}{2-\beta}\right)^\beta. \tag{18}$$

Therefore, by means of Theorem 3, we establish the global asymptotic stability of the zero solution. Consequently, the drive-response maps (1) are globally $Q - S$ synchronized in dimension m. □

4. Q–S Synchronization in Dimension n

Let us now move to establish $Q - S$ synchronization in dimension n. In this section, we assume $n < m$. We define the following notations:

$$\begin{aligned}
\mathbf{Q} &\in \mathbb{R}^{n\times m}, \\
\mathbf{q} &: \mathbb{R}^m \longrightarrow \mathbb{R}^n, \\
\text{and } S &: \mathbb{R}^n \longrightarrow \mathbb{R}^n.
\end{aligned} \tag{19}$$

We set the last $m-n$ controller components to zero, i.e.,

$$u_i = 0 \quad \text{for } n < i \le m. \tag{20}$$

Then, the error system reduces to

$$\begin{aligned} {}^{C}\Delta^{\beta} e(t) &= \mathbf{Q}BY(t+\beta-1) + \mathbf{Q}g(Y(t+\beta-1)) + \widehat{\mathbf{Q}} \\ &\quad \times \widehat{U} + {}^{C}\Delta^{\beta}\mathbf{q}(Y(t)) - {}^{C}\Delta^{\beta}S(X(t)), \end{aligned} \tag{21}$$

where $\widehat{\mathbf{Q}}$ is an invertible $n \times n$ matrix and $\widehat{U} = (u_1, \ldots, u_n)^T$. This can be further simplified to

$${}^{C}\Delta^{\beta} e(t) = (A-L)e(t) + \mathbf{T} + \widehat{\mathbf{Q}} \times \widehat{U}, \tag{22}$$

where $L \in \mathbb{R}^{n\times n}$ is an appropriate control matrix and

$$\begin{aligned} \mathbf{T} &= (L-A)e(t) + \mathbf{Q}BY(t) + \mathbf{Q}g(Y(t)) \\ &\quad + {}^{C}\Delta^{\beta}\mathbf{q}(Y(t)) - {}^{C}\Delta^{\beta}S(X(t)). \end{aligned} \tag{23}$$

To achieve Q–S synchronization between the drive-response maps (1) in dimension n, we propose choosing

$$\widehat{U} = -\widehat{\mathbf{Q}}^{-1}\mathbf{T}. \tag{24}$$

Substituting (24) into (22) yields the error dynamics

$${}^{C}\Delta^{\beta} e(t) = (A-L)e(t+\beta-1). \tag{25}$$

The following theorem can be proven in the exact same way as Theorem 4.

Theorem 5. *By selecting control matrix L such that all the eigenvalues λ of matrix $A-L$ satisfy $-2^{\beta} < \lambda < 0$, the drive and response maps (1) are globally Q–S synchronized in n dimensions subject to (20) and (24).*

5. Numerical Examples

In order to show the validity of the proposed control strategies, let us consider some numerical examples. The 2D fractional Hénon map given by

$$\begin{aligned} {}^{C}\Delta^{\alpha} x_1(t) &= x_2(t+\alpha-1) + 1 - a_1 x_1^2(t+\alpha-1) \\ &\quad - x_1(t+\alpha-1), \\ {}^{C}\Delta^{\alpha} x_2(t) &= b_1 x_1(t+\alpha-1) - x_2(t+\alpha-1), \end{aligned} \tag{26}$$

is chosen as the driving map. The fractional Hénon map (26) was proposed in [34]. The authors showed that this map has a chaotic attractor, for instance, when $(a_1, b_1) = (1.4, 0.3)$ and $\alpha = 0.984$. In order to unify the notation, (26) can be rewritten as

$${}^{C}\Delta^{\alpha} X(t) = AX(t) + f(X(t)), \tag{27}$$

where

$$\begin{aligned} A &= \begin{pmatrix} -1 & 1 \\ b_1 & -1 \end{pmatrix} \\ \text{and } f &= \begin{pmatrix} 1 - a_1 x_1^2(t) \\ 0 \end{pmatrix}. \end{aligned} \tag{28}$$

The chaotic behavior of the drive map is depicted in Figure 1.

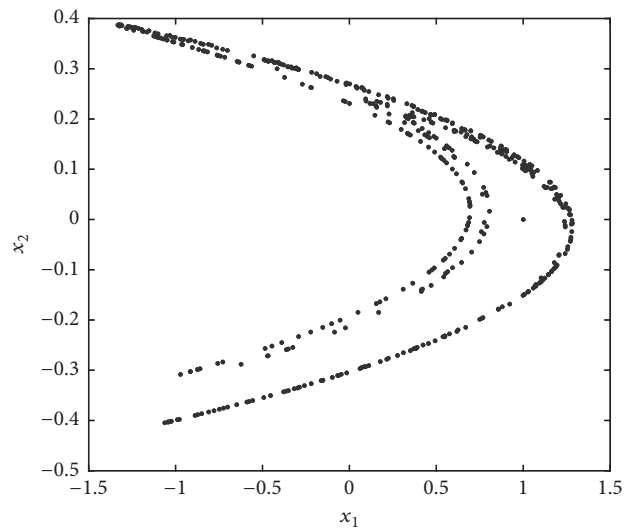

Figure 1: Phase space plot for the fractional Hénon map with $(a_1, b_1) = (1.4, 0.3)$, $\alpha = 0.984$, and $x_1(0) = x_2(0) = 0$.

As for the response map, we choose the 3D fractional-order generalized Hénon map [35], which is of the following form:

$$\begin{aligned} {}^{C}\Delta^{\beta} y_1(t) &= -y_1(t+\beta-1) - b_2 y_3(t+\beta-1) \\ &\quad + u_1(t+\beta-1), \\ {}^{C}\Delta^{\beta} y_2(t) &= b_2 y_3(t+\beta-1) + y_1(t+\beta-1) \\ &\quad - y_2(t+\beta-1) + u_2(t+\beta-1), \\ {}^{C}\Delta^{\beta} y_3(t) &= 1 + y_2(t+\beta-1) - a_2 y_3^2(t+\beta-1) \\ &\quad - y_3(t+\beta-1) + u_3(t+\beta-1). \end{aligned} \tag{29}$$

This system exhibits a chaotic behavior subject to certain conditions. We choose as an example the parameters $(a_2, b_2) = (0.99, 0.2)$ and $\beta = 0.984$, which has chaotic trajectories as shown in Figure 2. Map (29) can be rewritten as

$${}^{C}\Delta^{\beta} Y(t) = BY(t) + g(Y(t)), \tag{30}$$

where

$$\begin{aligned} B &= \begin{pmatrix} -1 & 0 & -b_2 \\ 1 & -1 & b_2 \\ 0 & 1 & -1 \end{pmatrix} \\ \text{and } g &= \begin{pmatrix} 0 \\ 0 \\ 1 - a_2 y_3^2(t) \end{pmatrix}. \end{aligned} \tag{31}$$

We will take 3- and 2-dimensional Q–S synchronization cases separately following the control laws of Theorems 4 and 5, respectively.

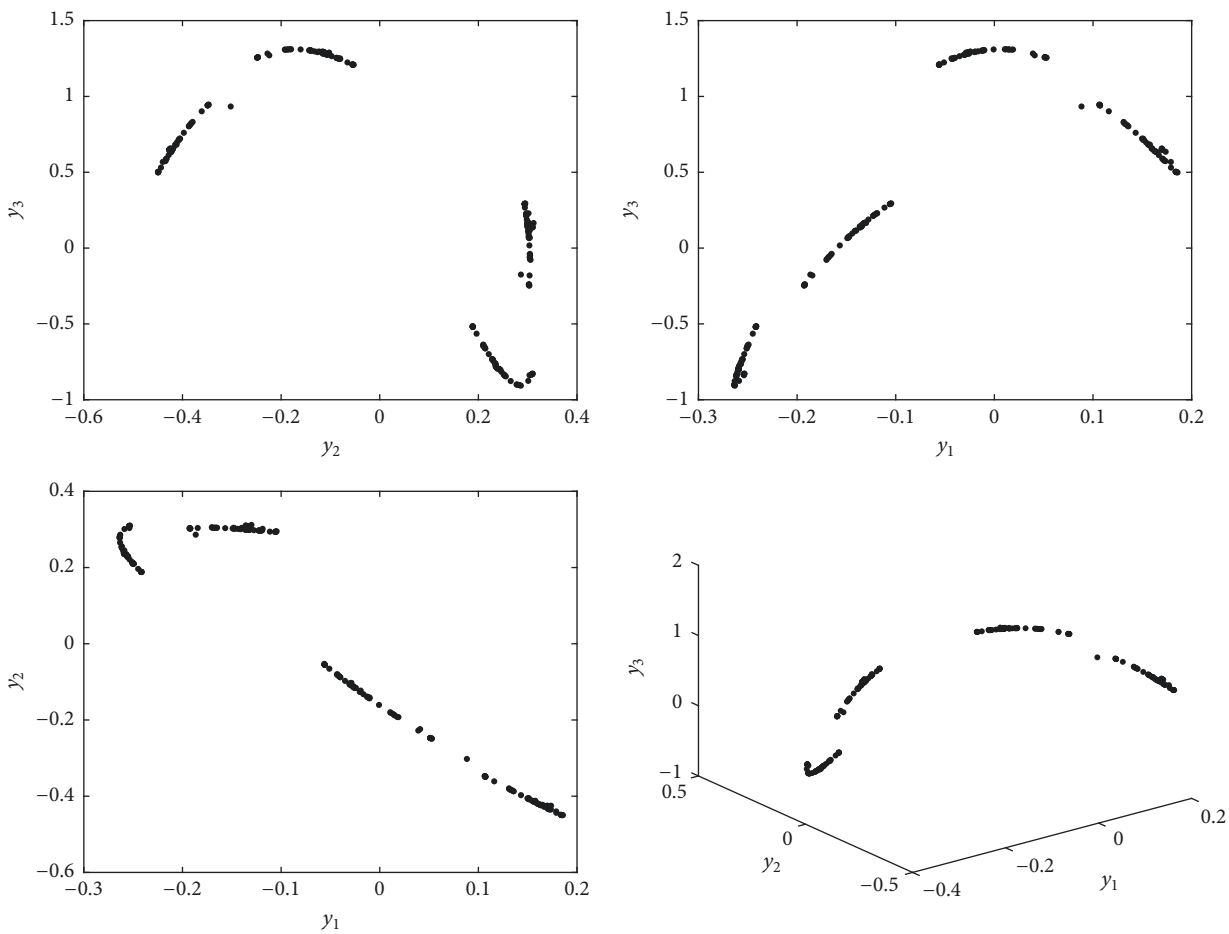

Figure 2: Phase portraits for the fractional generalized Hénon map with $(a_2, b_2) = (0.99, 0.2)$, $\beta = 0.984$ and $(y_1(0), y_2(0), y_3(0)) = (0.1, 0.2, 0.5)$.

Case 1. Let us, first, consider the 3-dimensional Q–S synchronization case. Based on the approach stated in Section 3, the error system is given by

$$\begin{aligned}(e_1(t), e_2(t), e_3(t))^T &= Q(y_1(t), y_2(t), y_3(t)) \\ &\quad - S(x_1(t), x_2(t)),\end{aligned} \tag{32}$$

where

$$\begin{aligned}&Q(y_1(t), y_2(t), y_3(t)) \\ &\quad = (y_1(t), y_1(t) + y_2(t), y_3(t)(3 + y_2(t)))^T,\end{aligned} \tag{33}$$

and

$$S(x_1(t), x_2(t)) = (x_1(t), x_2(t), x_1(t) + x_2(t)). \tag{34}$$

We may rewrite Q in the following form:

$$\begin{aligned}&Q(y_1(t), y_2(t), y_3(t)) \\ &\quad = \mathbf{Q} \times (y_1(t), y_2(t), y_3(t))^T \\ &\quad + \mathbf{q}(y_1(t), y_2(t), y_3(t))\end{aligned} \tag{35}$$

where

$$\mathbf{Q} = \begin{pmatrix} 1 & 0 & 0 \\ 1 & 2 & 0 \\ 0 & 0 & 3 \end{pmatrix} \tag{36}$$

and

$$\mathbf{q}(y_1(t), y_2(t), y_3(t)) = (0, 0, y_2(t)\, y_3(t))^T. \tag{37}$$

It is easy to see that

$$\mathbf{Q}^{-1} = \begin{pmatrix} 1 & 0 & 0 \\ -\frac{1}{2} & \frac{1}{2} & 0 \\ 0 & 0 & \frac{1}{3} \end{pmatrix}. \tag{38}$$

According to our approach described in Section 3, there exists a control matrix C such that all the eigenvalues $B - C$ satisfy the condition of Theorem 4. We may simply choose the following:

$$C = \begin{pmatrix} 0 & 0 & 0 \\ 1 & 0 & 0 \\ 0 & 1 & 0 \end{pmatrix}. \tag{39}$$

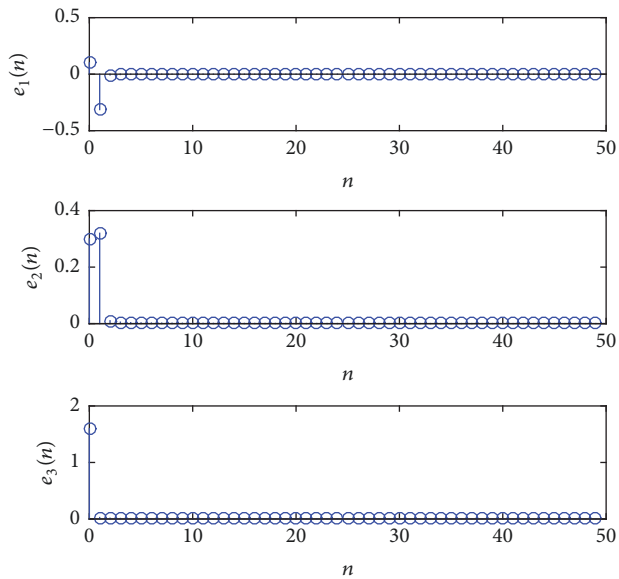

Figure 3: The evolution of errors over time for Case 1.

We start by calculating $\mathbf{R}$ by means of (11) and then U by means of (14). The resulting error system is given by

$$\begin{aligned} {}^{C}\Delta^{\beta} e_1(t) &= -e_1(t+\beta-1) - b_2 e_3(t+\beta-1), \\ {}^{C}\Delta^{\beta} e_2(t) &= -e_2(t+\beta-1) + b_2 e_3(t+\beta-1), \\ {}^{C}\Delta^{\beta} e_3(t) &= -e_3(t+\beta-1). \end{aligned} \tag{40}$$

The time evolution of the errors is depicted in Figure 3 for the initial values:

$$\begin{pmatrix} e_1(0) \\ e_2(0) \\ e_3(0) \end{pmatrix} = \begin{pmatrix} 0.1 \\ 0.3 \\ 1.6 \end{pmatrix}. \tag{41}$$

The errors clearly converge to zero in sufficient time indicating that the drive map (26) and the response map (29) become Q–S synchronized in 3 dimensions.

Case 2. As for the two-dimensional case, we follow the approach described in Section 4. The error system is given by

$$\begin{aligned} &(e_1(t), e_2(t), e_3(t))^T \\ &\quad = Q(y_1(t), y_2(t), y_3(t)) - S(x_1(t), x_2(t)), \end{aligned} \tag{42}$$

where

$$\begin{aligned} &Q(y_1(t), y_2(t), y_3(t)) \\ &\quad = \left(y_1(t) + 2y_2(t) + y_3^2(t), -y_1(t) + 3y_3(t)\right)^T, \end{aligned} \tag{43}$$

and

$$S(x_1(t), x_2(t)) = (x_1(t), x_1(t)x_2(t)). \tag{44}$$

We can write

$$\begin{aligned} &Q(y_1(t), y_2(t), y_3(t)) \\ &\quad = \mathbf{Q} \times (y_1(t), y_2(t), y_3(t))^T \\ &\qquad + \mathbf{q}(y_1(t), y_2(t), y_3(t)), \end{aligned} \tag{45}$$

where

$$\mathbf{Q} = \begin{pmatrix} 1 & 2 & 0 \\ -1 & 0 & 3 \end{pmatrix}, \tag{46}$$

and

$$\mathbf{q}(y_1(t), y_2(t), y_3(t)) = \left(y_3^2(t), 0\right)^T. \tag{47}$$

This yields

$$\begin{aligned} \widehat{\mathbf{Q}} &= \begin{pmatrix} 1 & 2 \\ -1 & 0 \end{pmatrix} \\ \text{and } \widehat{\mathbf{Q}}^{-1} &= \begin{pmatrix} 1 & 2 \\ -1 & 0 \end{pmatrix}. \end{aligned} \tag{48}$$

According to Theorem 5, the control matrix L can be selected as

$$L = \begin{pmatrix} 0 & 1 \\ -1 + b_1 & -\frac{1}{2} \end{pmatrix}, \tag{49}$$

which clearly satisfies the condition of Theorem 5. Next, we calculate $\mathbf{T}$ as specified in (23) and $\widehat{U}$ as in (24). The complete control vector U is formed by appending a zero to the end of $\widehat{U}$. The resulting error system is given by

$$\begin{aligned} {}^{C}\Delta^{\beta} e_1(t) &= -e_1(t+\beta-1), \\ {}^{C}\Delta^{\beta} e_2(t) &= e_1(t+\beta-1) - \frac{1}{2} e_2(t+\beta-1). \end{aligned} \tag{50}$$

The convergence of the errors to zero is depicted in Figure 4 for the initial conditions:

$$\begin{pmatrix} e_1(0) \\ e_2(0) \end{pmatrix} = \begin{pmatrix} 0.75 \\ 1.14 \end{pmatrix}. \tag{51}$$

6. Concluding Remarks

This paper has studied Q–S synchronization of fractional-order discrete-time chaotic systems of different dimensions. The Q–S scheme aims for the general definition of the error towards zero in finite time, thereby covering a range of different synchronization types. We assume an n-dimensional drive map and an m-dimensional response map with the condition $m > n$. Two different control laws have been derived and the asymptotic stability of their zero solution investigated through the linearization method. The two strategies correspond to the synchronization dimensions $d = n$ and $d = m$.

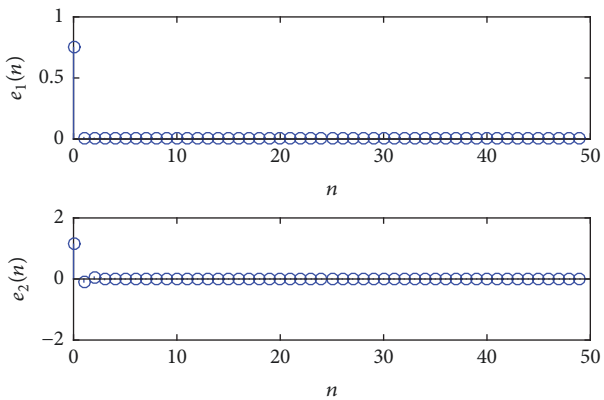

Figure 4: The evolution of errors over time for Case 2.

Computer simulation results have been presented, whereby a 3-dimensional fractional-order generalized Hénon map response synchronized the 2-dimensional fractional-order Hénon drive. The two proposed schemes were utilized to achieve 2- and 3-dimensional synchronization. The errors have been shown to converge towards zero in sufficient time.

Data Availability

No external data has been used in this manuscript.

Conflicts of Interest

The authors declare that they have no conflicts of interest.

References

[1] M. Hénon, "A two-dimensional mapping with a strange attractor," *Communications in Mathematical Physics*, vol. 50, no. 1, pp. 69–77, 1976.

[2] R. LOZI, "Un atracteur étrange du type attracteur de H énon," *Le Journal de Physique Colloques*, vol. 39, pp. 9-10, 1978.

[3] M. Itoh, T. Yang, and L. O. Chua, "Conditions for impulsive synchronization of chaotic and hyperchaotic systems," *International Journal of Bifurcation and Chaos*, vol. 11, no. 2, pp. 551–560, 2001.

[4] D. L. Hitzl and F. Zele, "An exploration of the Hénon quadratic map," *Physica D: Nonlinear Phenomena*, vol. 14, no. 3, pp. 305–326, 1985.

[5] K. Stefański, "Modelling Chaos and Hyperchaos with 3-D Maps," *Chaos, Solitons & Fractals*, vol. 9, no. 1, pp. 83–93, 1998.

[6] K. S. Miller and B. Ross, "Fractional difference calculus," in *Proceedings of the Int. Symp. Univalent Func., Frac. Calc. Appl.*, Ellis Horwood Ser. Math., pp. 139–152, Horwood, Chichester, 1989.

[7] F. M. Atici and P. W. Eloe, "Discrete fractional calculus with the nabla operator," *Electronic Journal of Qualitative Theory of Differential Equations*, no. 3, pp. 1–12, 2009.

[8] T. Abdeljawad, "On Riemann and Caputo fractional differences," *Computers & Mathematics with Applications*, vol. 62, no. 3, pp. 1602–1611, 2011.

[9] M. Holm, *The theory of discrete fractional calculus: Development and application, PhD thesis*, University of Nebraska-Lincoln, Lincoln, Nebraska, 2011.

[10] C. Goodrich and A. C. Peterson, *Discrete Fractional Calculus*, Springer International, New York, NY, USA, 2015.

[11] G. A. Anastassiou, "Principles of delta fractional calculus on time scales and inequalities," *Mathematical and Computer Modelling*, vol. 52, no. 3-4, pp. 556–566, 2010.

[12] M. Wyrwas, D. Mozyrska, and E. Girejko, "Stability of discrete fractional-order nonlinear systems with the nabla Caputo difference," in *Proceedings of the 6th Workshop on Fractional Differentiation and Its Applications, FDA 2013*, pp. 167–171, France, February 2013.

[13] G. Wu and D. Baleanu, "Discrete fractional logistic map and its chaos," *Nonlinear Dynamics*, vol. 75, no. 1-2, pp. 283–287, 2014.

[14] G. C. Wu, D. Baleanu, and S. D. Zeng, "Discrete chaos in fractional sine and standard maps," *Physics Letters A*, vol. 378, no. 5-6, pp. 484–487, 2014.

[15] Y. Liu, "Discrete Chaos in Fractional Henon Maps," *International Journal of Nonlinear Science*, vol. 18, no. 3, pp. 170–175, 2014.

[16] C. X. Liu, L. L. Huang, and K. T. Wu, "Chaos in discrete fractional cubic logistic map and bifurcation analysis," *J. Comput. Complex. Appl*, vol. 1, no. 2, pp. 105–111, 2015.

[17] L. M. Pecora and T. L. Carroll, "Synchronization in chaotic systems," *Physical Review Letters*, vol. 64, no. 8, pp. 821–824, 1990.

[18] A. Ouannas, A. T. Azar, and R. Abu-Saris, "A new type of hybrid synchronization between arbitrary hyperchaotic maps," *International Journal of Machine Learning and Cybernetics*, vol. 8, no. 6, pp. 1887–1894, 2017.

[19] A. Ouannas and Z. Odibat, "Generalized synchronization of different dimensional chaotic dynamical systems in discrete time," *Nonlinear Dynamics*, vol. 81, no. 1-2, pp. 765–771, 2015.

[20] A. Ouannas and G. Grassi, "Inverse full state hybrid projective synchronization for chaotic maps with different dimensions," *Chinese Physics B*, vol. 25, no. 9, Article ID 090503, 2016.

[21] G. C. Wu and D. Baleanu, "Chaos synchronization of the discrete fractional logistic map," *Signal Processing*, vol. 102, pp. 96–99, 2014.

[22] G.-C. Wu, D. Baleanu, H.-P. Xie, and F.-L. Chen, "Chaos synchronization of fractional chaotic maps based on the stability condition," *Physica A: Statistical Mechanics and its Applications*, vol. 460, pp. 374–383, 2016.

[23] Y. Liu, "Chaotic synchronization between linearly coupled discrete fractional Hénon maps," *Indian Journal of Physics*, vol. 90, no. 3, pp. 313–317, 2016.

[24] O. Megherbi, H. Hamiche, S. d. Djennoune, and M. Bettayeb, "A new contribution for the impulsive synchronization of fractional-order discrete-time chaotic systems," *Nonlinear Dynamics*, vol. 90, no. 3, pp. 1519–1533, 2017.

[25] Z. Yan, "Q-S (lag or anticipated) synchronization backstepping scheme in a class of continuous–time hyperchaotic systems: a symbolic-numeric computation approach," *Chaos*, vol. 15, no. 2, 2005.

[26] Z. Yan, "Q-S synchronization in 3D Hénon-like map and generalized Hénon map via a scalar controller," *Physics Letters A*, vol. 342, no. 4, pp. 309–317, 2005.

[27] H. Manfeng and X. Zhenyuan, "A general scheme for Q-S synchronization of chaotic systems," *Nonlinear Analysis. Theory, Methods & Applications*, vol. 69, no. 4, pp. 1091–1099, 2008.

[28] J. Zhao and T. Ren, "Q–S synchronization between chaotic systems with double scaling functions," *Nonlinear Dynamics*, vol. 62, no. 3, pp. 665–672, 2010.

[29] J. Zhao and K. Zhang, "A general scheme for Q-S synchronization of chaotic systems with unknown parameters and scaling functions," *Applied Mathematics and Computation*, vol. 216, no. 7, pp. 2050–2057, 2010.

[30] A. Ouannas, A. T. Azar, and S. Vaidyanathan, "On a simple approach for Q-S synchronisation of chaotic dynamical systems in continuous-time," *International Journal of Computational Science and Mathematics*, vol. 8, no. 1, pp. 20–27, 2017.

[31] A. Ouannas and R. Abu-Saris, "A robust control method for QS synchronization between different dimensional integer-order and fractional-order chaotic systems," *J. Cont. Sci. Eng*, pp. 1–7, 2015.

[32] A. Ouannas, A. T. Azar, T. Ziar, and S. Vaidyanathan, "Q-S chaos synchronization between fractional–order master and integer–order slave systems," in *Proceedings of the 15th Int. Multi-Conf. Sys. Sig. Dev.*, 2018.

[33] J. Cermák, I. Gyõri, and L. e. Nechvátal, "On explicit stability conditions for a linear fractional difference system," *Fractional Calculus and Applied Analysis*, vol. 18, no. 3, pp. 651–672, 2015.

[34] T. Hu, "Discrete Chaos in Fractional Henon Map," *Appl. Math*, vol. 5, pp. 2243–2248, 2014.

[35] M. K. Shukla and B. B. Sharma, "Investigation of chaos in fractional order generalized hyperchaotic Henon map," *AEÜ - International Journal of Electronics and Communications*, vol. 78, pp. 265–273, 2017.